Steel and Composite Structures, *Vol. 21, No. 3 (2016) 629-659*
DOI: http://dx.doi.org/10.12989/scs.2016.21.3.629

Web crippling strength of cold-formed stainless steel lipped channel-sections with web openings subjected to interior-one-flange loading condition

Amir M. Yousefi [1a], James B.P. Lim [*1], Asraf Uzzaman [2b], Ying Lian [3c], G. Charles Clifton [1d] and Ben Young [4e]

[1] *Department of Civil and Environmental Engineering, The University of Auckland, New Zealand*
[2] *Department of Mechanical and Aerospace Engineering, The University of Strathclyde, 75 Montrose Street, Glasgow G1 1XJ, UK*
[3] *SPACE, David Keir Building, Queen's University, Belfast, BT9 5AG, UK*
[4] *Department of Civil Engineering, The University of Hong Kong, Pokfulam Road, Hong Kong*

(*Received March 07, 2016, Revised May 13, 2016, Accepted May 15, 2016*)

Abstract. In cold-formed stainless steel lipped channel-sections, web openings are becoming increasingly popular. Such openings, however, result in the sections becoming more susceptible to web crippling, especially under concentrated loads applied near the web opening. This paper presents the results of a finite element parametric study into the effect of circular web openings on the web crippling strength of cold-formed stainless steel lipped channel-sections for the interior-one-flange (IOF) loading condition. This involves a bearing load applied to the top flange of a length of member, away from the end supports. The cases of web openings located centred beneath the bearing load (i.e. beneath the bearing plate delivering the load) and offset to the bearing plate, are considered. Three grades of stainless steel are considered: duplex EN1.4462, austenitic EN1.4404 and ferretic EN1.4003. In total, 2218 finite element models were analyzed. From the results of the parametric study, strength reduction factors for load bearing capacity are determined, where these reduction factors are applied to the bearing capacity calculated for a web without openings, to take account the influence of the web openings. The strength reduction factors are first compared to equations recently proposed for cold-formed carbon steel lipped channel-sections. It is shown that for the case of the duplex grade, the strength reduction factor equations for cold-formed carbon steel are conservative but only by 2%. However, for the cases of the austentic and ferritic grades, the cold-formed carbon steel equations are around 9% conservative. New strength reduction factor equations are proposed for all three stainless steel grades.

Keywords: cold-formed stainless steel; lipped channel-section; web crippling; finite element analysis; strength reduction factor

∗Corresponding author, Senior Lecturer, E-mail: james.lim@auckland.ac.nz
[a] Ph.D. Student, E-mail: ayou561@aucklanduni.ac.nz
[b] Research Fellow, E-mail: asraf.uzzaman@strath.ac.uk
[c] Ph.D. Student, E-mail: ylian01@qub.ac.uk
[d] Associate Professor, E-mail: c.clifton@auckland.ac.nz
[e] Professor, E-mail: young@hku.hk

Copyright © 2016 Techno-Press, Ltd.
http://www.techno-press.org/?journal=scs&subpage=6 ISSN: 1229-9367 (Print), 1598-6233 (Online)

1. Introduction

The use of cold-formed stainless steel in structural applications is growing steadily (Dai and Lam 2010, Theofanous and Gardner 2011, Kiymaz and Seckin 2014) and the use of web openings in such sections is becoming increasingly popular (Lawson *et al*. 2015) (see Fig. 1). Such openings, however, result in the sections being more susceptible to web crippling, especially under concentrated loads applied to the bearing flange in the vicinity of the openings. No previous research has considered the web crippling strength of cold-formed stainless steel lipped channel-sections with circular web openings under either of the one or two-flange loading conditions (see Figs. 2 and 3 for the interior-one-flange (IOF) loading condition). For cold-formed stainless steel lipped channel-sections without openings, only Kroyink *et al*. (1996) has considered the web crippling strength. More recently, Zhou and Young (2006, 2007, 2013) have considered the web crippling strength of cold-formed stainless steel tubular sections. Research by Lawson *et al*. (2015), while concerned with circular web openings, focussed on the bending strength of the sections and not on the web crippling strength under concentrated loads.

For cold-formed carbon steel lipped channel-sections, Lian (Lian *et al*. 2016a, b, c, d, Lian 2016) recently proposed strength reduction factor equations for sections with circular web openings under one-flange loading; the cases of both flanges fastened and flanges unfastened to the bearing plates were considered. The work of Lian (Lian *et al*. 2016a, b, c, d, Lian 2016) was a continuation of that of Uzzaman *et al*. (2012a, b, c, 2013), who considered two-flange loading. The strength reduction factor equations proposed were determined from a parametric study using the finite element program ABAQUS (2014); laboratory test results were used to validate the finite element models. Other recent work reported in the literature includes that of Natário *et al*. (2015), who proposed a Direct Strength Method (DSM) approach to predict the web crippling strength of cold-formed carbon steel beams under end-two-flange (ETF) loading condition, and Sudarajah *et al*. (2016) who reported experimental tests and finite element analysis for lipped channel beams (LCBs) under two flange loading conditions.

This paper considers how applicable the equations proposed by Lian (Lian *et al*. 2016a, b, Lian 2016) for the interior-one-flange (IOF) loading (see Fig. 2), are to three stainless steel grades:

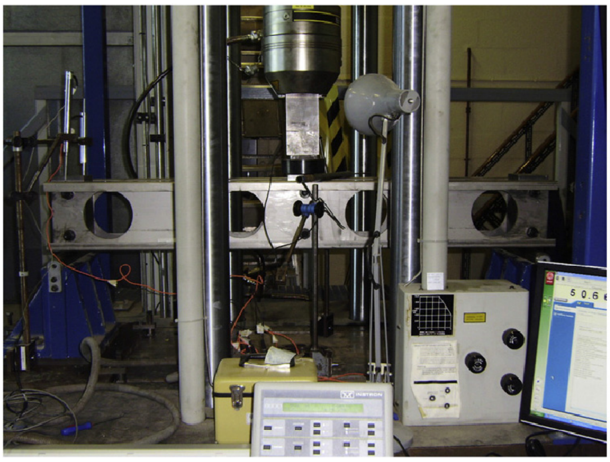

Fig. 1 Photograph of cold-formed stainless steel lipped channel-sections with circular web openings after Lawson *et al*. (2015)

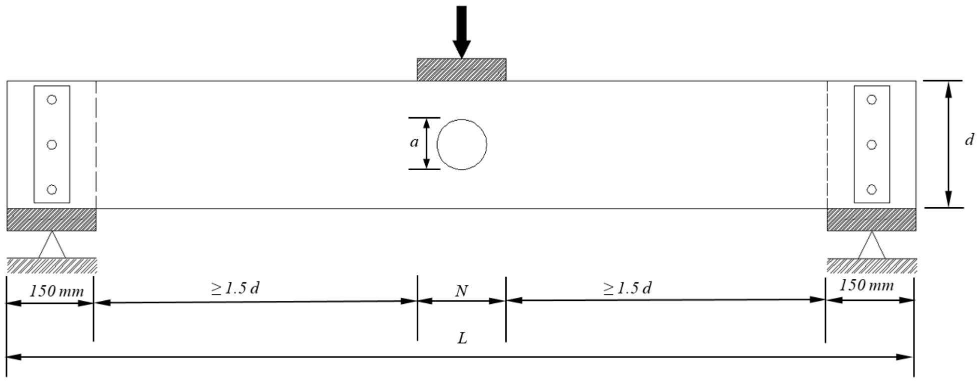

(a) With circular web opening centred under bearing plate

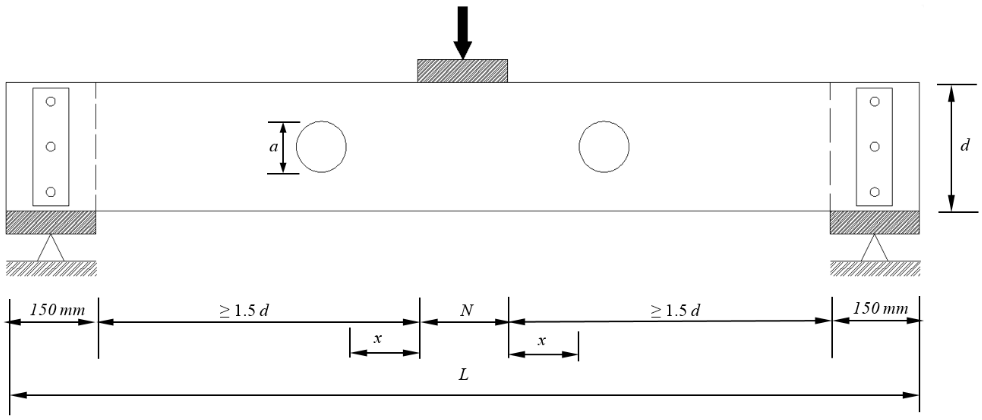

(b) With circular web openings offset from bearing plate

Fig. 2 Interior-one-flange (IOF) loading condition after Lian (Lian *et al*. 2016a, b, Lian 2016)

duplex grade EN 1.4462; austenitic grade 1.4404 and ferritic grade 1.4003. Typical stress-strain curves for the three grades were taken from Chen and Young (2006) and Arrayago *et al*. (2015). Comparative hot-rolled steel stress strain curves can be found in Yousefi *et al*. (2014) and Rezvani *et al*. (2015).

2. Experimental investigation and finite element modelling

For cold-formed carbon steel, Lian (Lian *et al*. 2016a, b, Lian 2016) recently conducted 43 interior-one-flange (IOF) laboratory tests on lipped channel-sections with circular web openings subjected to web crippling (see Fig. 3). Fig. 4 shows the definition of the symbols used to describe the dimensions of the cold-formed carbon steel lipped channel-sections considered in the test programme. The laboratory tests were used to validate a non-linear geometry elasto-plastic finite element model in ABAQUS (2014), which was then used for a parametric study, from which design recommendations were proposed in the form of strength reduction factor equations, relating the loss of strength due to the web openings to the strength of the web without openings. The size of the circular web openings was varied in order to investigate the effect of the web opening size

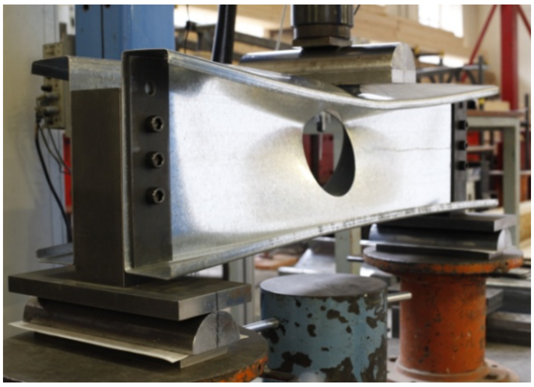

(a) Centred circular web opening

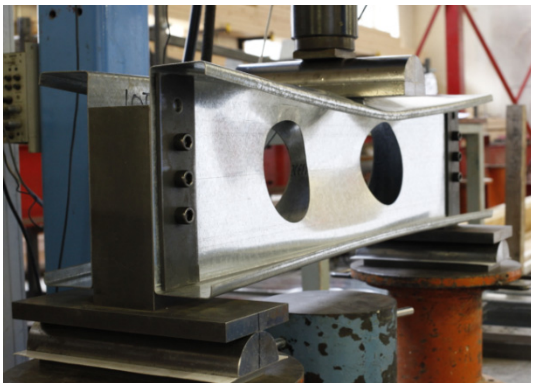

(b) Offset circular web opening

Fig. 3 Experimental analysis of cold-formed steel lipped channel-sections under interior-one-flange (IOF) loading condition for the case of flange unfastened to bearing plate after Lian (Lian *et al*. 2016a, b, Lian 2016)

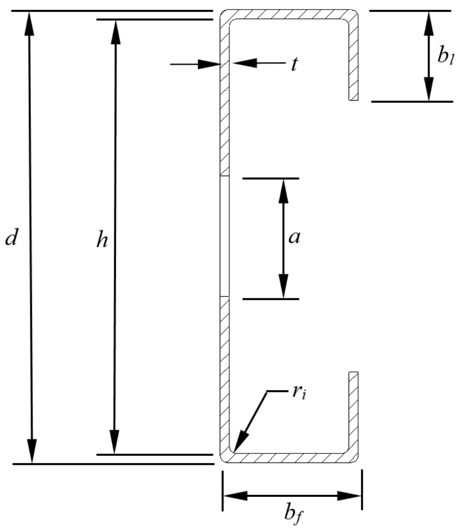

Fig. 4 Definition of symbols

on the web crippling strength. Full details of both the laboratory tests and finite element models (see Fig. 5) can be found in Lian *et al*. (2016a, b, e). However, brief details of the finite element models are summarised below.

In the finite element model, one-quarter of the test set-up of Lian *et al*. (2016a, b, e) was modelled, as shown in Fig. 5. In ABAQUS, the S4R shell element was used. The S4R is a four-node double curved thin or thick shell element with reduced integration and finite membrane strains. The S4R has six degrees of freedom per node and provides accurate solutions to most applications. The bearing plates and load transfer block were modelled using analytical rigid plates and using C3D8R element, which is suitable for three-dimensional modelling of structures with plasticity, stress stiffening, large deflection, and large strain capabilities. The solid element is defined by eight nodes having three translational degrees of freedom at each node.

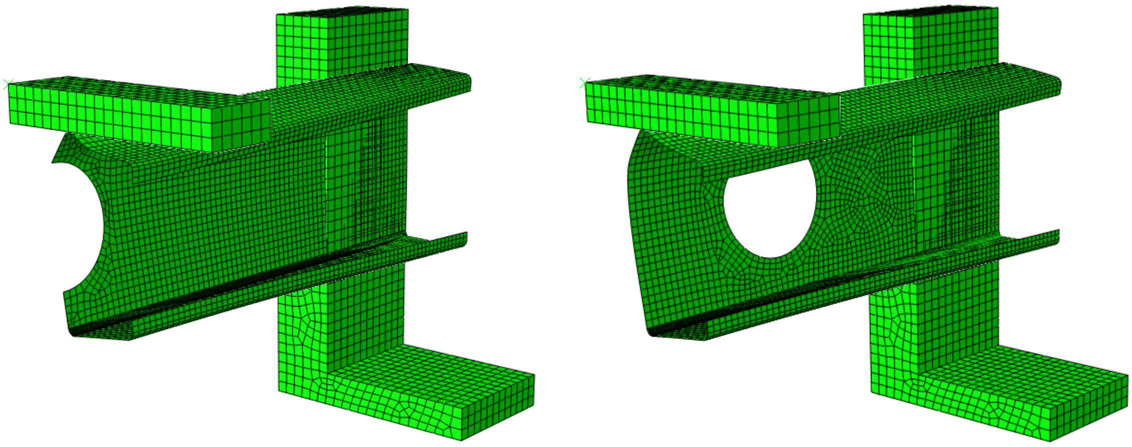

(a) Centred circular web opening (b) Offset circular web opening

Fig. 5 Deformed shape predicted from finite element analysis of cold-formed steel lipped channel-sections under interior-one-flange (IOF) loading condition for case of flange unfastened to bearing plate after Lian (Lian *et al*. 2016a, b, Lian 2016)

Contact between the bearing plate, the load transfer block and the cold-formed steel section was modelled in ABAQUS using the contact pairs option. The two contact surfaces were not allowed to penetrate each other. No friction was modelled between the surfaces. The lipped channel-sections of the model were based on the centreline dimensions of the cross-sections. Finite element mesh sizes were 5 mm × 5 mm for the cold-formed steel channel sections and 8 mm × 8 mm for the bearing plates and load transfer blocks. The vertical load applied to the channel section through the bearing plate in the laboratory tests was modelled using displacement control. In the finite element model, a displacement in the vertical y direction was applied to the reference point of the analytical rigid plate that modelled the bearing plate. At the line of symmetry of the channel section, all nodes were restrained in the z direction and rotation about x and y axes. The nodes on symmetry surface of load transfer block were prevented from translational axes in the x direction and rotation about the y and z axes. The channel section specimens were tested in pairs, which were bolted to load transfer blocks at each end of the specimens through the web by a vertical row of M16 high tensile bolts. In the shell element idealisation, cartesian connectors with an in-plane stiffness were used to simulate bolt-hole elongation instead of physically modelling bolts and holes. "CONN3D2" connector elements were used to model the in-plane translational stiffness i.e., y- and z-directions. The stiffness of the connectors element was 10 kN/mm, which Lim and Nethercot (2001) suggest would be suitable. In the x direction, the nodes were prevented from translating.

The models have been coded such the nominal dimension of the model and the length of the bearing plate as well as the ratio of the diameter of the circular web openings to the depth of the flat portion of the webs (a / h) can be determined from the coding system. As an example, the label "142-N100-A0.2-FR" means the following. The first notation is the nominal depth of the models in millimeters. The notation "*N100*" indicates the length of bearing in millimeters (i.e., 100 mm). The notation "*A0.2*" indicates the ratio of the diameter of the openings to the depth of the flat portion of the webs (a / h) and are one of 0.2, 0.4, 0.6 and 0.8 (i.e., *A0.2* means a/h = 0.2; *A0.4* means a / h = 0.4 etc). Plain lipped channel-sections (i.e., without circular web openings) are

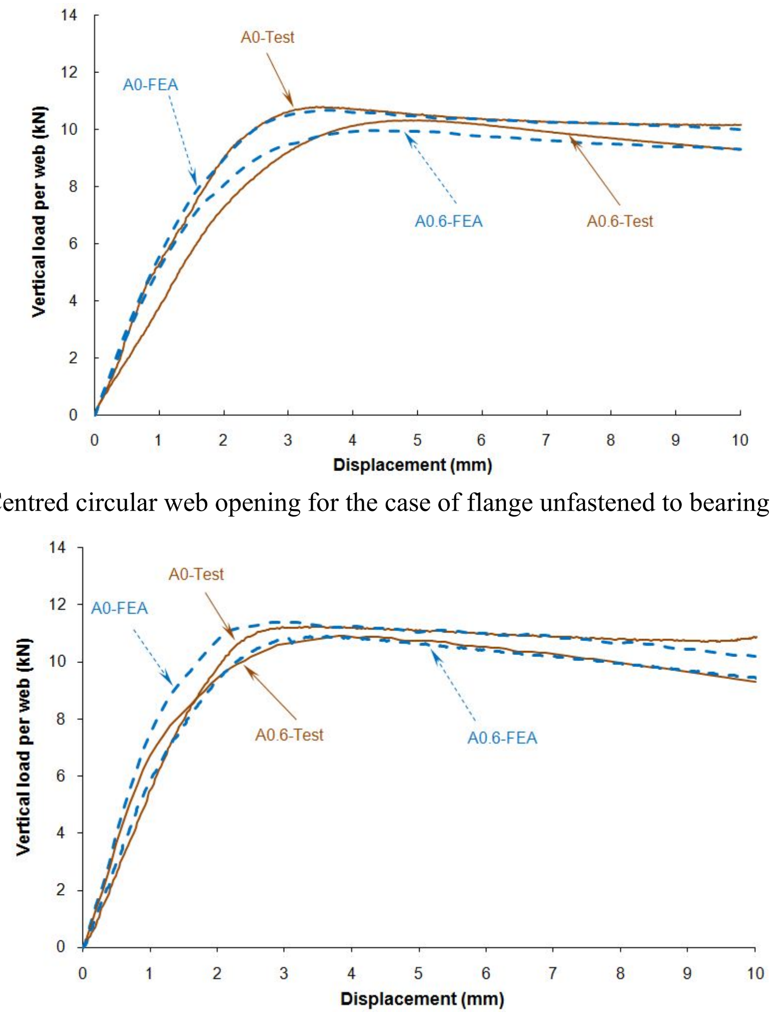

(b) Offset circular web opening for the case of flange fastened to bearing plate

Fig. 6 Comparison of finite element results and experimental test results (Lian *et al*. 2016a, b, Lian 2016)

denoted by "*A0*". The flange unfastened and fastened cases are identified as "*FR*" and "*FX*", respectively.

Fig. 6 compares the experimental and numerical load-displacement curves for a cold-formed carbon steel lipped channel-section, 142×60×13-t1.3-N100-FR, covering the cases both with and without the circular web openings. As can be seen, there is good agreement between the failure loads of the tested specimens and the finite element results.

For cold-formed stainless steel lipped channel-sections, the numerical failure loads with and without circular web openings were then determined for the three stainless steel grades: duplex grade EN 1.4462; austenitic grade 1.4404 and ferritic grade 1.4003 (see Table 1). These results were compared with the failure loads calculated in accordance with ASCE (2002), NAS (2007) and AS/NZS 4600 (2005) (see Table 2). The failure loads predicted from the finite element model are similar to the codified failure loads of the sections.

Table 1 Dimensions and web crippling strengths predicted from finite element analysis of cold-formed stainless steel lipped channel-sections

A. For the case of flange unfastened to the bearing plate

Specimen	Web	Flange	Lip	Thickness	Length	Web opening	Duplex			Ferritic			Austenitic		
	d (mm)	b_f (mm)	b_l (mm)	t (mm)	L (mm)	a (mm)	$P(A0)$ (kN)	$P(Opening)$ (kN)	$P(Opening)$ (kN)	$P(A0)$ (kN)	$P(Opening)$ (kN)	$P(Opening)$ (kN)	$P(A0)$ (kN)	$P(Opening)$ (kN)	$P(Opening)$ (kN)
								Offset	Centred		Offset	Centred		Offset	Centred
142-N100-MA0.6-FR	141.82	60.63	13.66	1.27	720.00	139.27	11.57	10.95	10.41	9.64	9.40	8.98	8.52	8.14	7.81
142-N120-MA0.6-FR	142.24	60.37	13.90	1.27	740.00	139.70	12.28	11.41	10.77	10.30	10.02	9.38	8.90	8.66	8.21
142-N150-MA0.4-FR	142.40	59.79	13.28	1.28	770.00	139.84	12.94	12.53	12.25	11.15	10.94	10.69	9.61	9.48	9.31
202-N100-MA0.4-FR	202.04	64.79	14.78	1.38	899.20	199.28	12.56	11.44	11.96	10.95	10.44	10.92	9.60	7.95	9.57
202-N100-MA0.6-FR	202.04	64.79	14.78	1.38	899.20	199.28	12.55	10.37	12.47	10.95	9.83	10.93	9.60	7.76	9.58
202-N120-MA0.4-FR	202.00	65.00	14.73	1.38	920.00	199.24	12.81	11.65	12.09	11.59	10.88	11.25	10.15	9.71	10.10
202-N120-MA0.6-FR	202.00	65.00	14.73	1.38	920.00	199.24	12.81	10.51	10.80	11.59	10.03	10.05	10.15	9.48	9.31
202-N150-MA0.4-FR	202.01	65.04	14.98	1.38	950.00	199.24	13.15	11.93	12.26	12.25	11.27	11.52	10.90	10.49	10.65
302-N100-MA0.6-FR	303.18	87.91	18.83	1.90	1200.00	299.37	24.63	21.36	24.63	20.65	18.81	20.60	18.40	16.64	18.36
302-N120-MA0.6-FR	303.07	87.95	18.26	1.90	1221.00	299.26	26.01	21.95	25.30	22.47	20.18	22.16	19.41	17.66	19.30
302-N150-MA0.6-FR	303.03	88.54	18.97	1.90	1249.00	299.23	27.71	22.58	27.51	24.65	21.50	24.55	21.50	19.26	21.45

Table 1 Dimensions and web crippling strengths predicted from finite element analysis of cold-formed stainless steel lipped channel-sections

B. For the case of flange fastened to the bearing plate

Specimen	Web	Flange	Lip	Thickness	Length	Web opening	Duplex			Ferritic			Austenitic		
	d (mm)	b_f (mm)	b_l (mm)	t (mm)	L (mm)	a (mm)	$P(A0)$ (kN)	$P(Opening)$ (kN)	$P(Opening)$ (kN)	$P(A0)$ (kN)	$P(Opening)$ (kN)	$P(Opening)$ (kN)	$P(A0)$ (kN)	$P(Opening)$ (kN)	$P(Opening)$ (kN)
								Offset	Centred		Offset	Centred		Offset	Centred
142-N100 -MA0.6-FX	142.49	60.33	13.79	1.29	720.00	139.27	12.76	12.53	11.66	10.13	10.15	9.67	9.40	9.24	8.64
142-N120 -MA0.6-FX	142.38	60.21	13.68	1.29	740.00	139.70	13.49	13.38	12.07	11.01	10.96	10.17	9.86	9.76	9.04
142-N150 -MA0.4-FX	142.18	60.12	13.19	1.28	770.00	139.84	14.37	14.34	13.80	11.91	11.91	11.64	10.70	10.47	10.46
202-N100 -MA0.4-FX	201.99	64.87	14.76	1.37	900.00	199.28	13.51	14.17	13.49	10.99	11.57	10.56	10.08	10.51	10.01
202-N100 -MA0.6-FX	201.99	64.87	14.76	1.37	900.00	199.28	13.51	14.03	12.60	10.99	11.50	10.47	10.08	10.38	9.88
202-N120 -MA0.4-FX	202.05	64.99	14.82	1.41	920.00	199.24	15.18	14.24	15.14	12.51	11.82	12.24	11.20	10.51	10.97
202-N120 -MA0.6-FX	202.05	64.99	14.82	1.41	920.00	199.24	15.18	14.06	13.60	12.51	11.70	11.90	11.20	10.39	10.71
202-N150 -MA0.4-FX	202.00	64.93	15.00	1.41	950.00	199.24	16.45	16.30	16.05	13.73	13.69	13.14	12.23	12.09	11.58
302-N100 -MA0.6-FX	303.20	88.24	18.66	1.96	1199.00	299.37	26.27	25.72	23.37	20.91	20.78	19.91	19.25	19.05	17.93
302-N120 -MA0.6-FX	303.50	88.53	18.36	1.93	1219.00	299.26	27.17	26.57	23.49	21.96	21.84	20.62	19.75	19.66	18.59
302-N150 -MA0.6-FX	303.85	88.71	18.41	1.90	1248.33	299.23	28.56	27.19	24.25	23.59	23.41	21.28	21.06	20.46	19.31

Table 2 Comparison of numerical results with design strength for the case of flange fastened to the bearing plate without circular web opening

Specimen	Web slender-ness	Bearing length to thickness ratio	Bearing length to web height ratio	Inside bend radius to thickness ratio	Failure load per web	Web crippling strength per web predicted from current design codes			Comparison		
	h/t	N/t	N/h	r_i/t	P_{FEA} (kN)	P_{NAS} (kN)	P_{ASCE} (kN)	$P_{AS/NZS}$	P/P_{NAS}	P/P_{ASCE}	$P/P_{AS/NZS}$
142×60×13 -t1.3-N100 -A0-FX	110.19	78.74	0.71	3.78	10.13	9.23	10.13	9.22	1.10	1.00	1.10
142×60×13 -t1.3-N120 -A0-FX	110.11	94.49	0.86	3.78	11.01	9.72	11.21	9.72	1.13	0.98	1.13
142×60×13 -t1.3-N150 -A0-FX	109.08	117.19	1.07	3.75	11.91	10.16	12.56	10.15	1.17	0.95	1.17
202×65×15 -t1.4-N100 -A0-FX	144.37	72.46	0.50	3.62	10.99	10.08	10.37	10.08	1.09	1.06	1.09
202×65×15 -t1.4-N120 -A0-FX	144.41	86.96	0.60	3.62	12.51	11.35	12.21	11.35	1.10	1.02	1.10
202×65×15 -t1.4-N150 -A0-FX	144.38	108.70	0.75	3.62	13.73	12.11	13.92	12.10	1.13	0.99	1.13
302×90×18 -t2.0-N100 -A0-FX	157.58	52.63	0.33	2.63	20.91	20.67	19.46	20.67	1.01	1.07	1.01
302×90×18 -t2.0-N120 -A0-FX	157.74	63.16	0.40	2.63	21.96	20.91	19.86	20.91	1.05	1.11	1.05
302×90×18 -t2.0-N150 -A0-FX	155.43	77.72	0.50	2.59	23.59	21.34	21.41	21.32	1.11	1.10	1.11
Mean, Pm									1.10	1.03	1.09
Coefficient of variation									0.09	0.05	0.04

3. Parametric study for stainless steel grades

In this study, in order to investigate the effect of circular web openings on the web crippling strength of cold-formed stainless steel lipped channel-sections, a total of 2218 finite element models of lipped channel-sections with various dimensions and thicknesses were considered for

Table 3 Web crippling strengths of duplex stainless steel sections predicted from finite element analysis

A. *a*/*h* for centred circular web opening case

Specimen	Thickness	Unfastened FEA load per web, P_{FEA}					Fastened FEA load per web, P_{FEA}				
	t	*A* (0)	*A* (0.2)	*A* (0.4)	*A* (0.6)	*A* (0.8)	*A* (0)	*A* (0.2)	*A* (0.4)	*A* (0.6)	*A* (0.8)
	(mm)	(kN)	(kN)	(kN)	(kN)	(kN)	(kN)	(kN)	(kN)	(kN)	(kN)
142-N100-FR	1.27	11.57	11.50	11.45	10.41	9.10	12.76	12.72	12.72	11.66	9.98
142-N100-FR	4.00	93.12	91.83	86.44	80.68	71.84	112.57	111.80	105.57	95.87	86.45
142-N100-FR	6.00	174.70	171.91	162.61	147.12	122.67	201.87	199.27	191.73	178.14	171.28
142-N120-FR	1.27	12.28	12.19	11.83	10.77	9.53	13.49	13.48	13.37	12.07	10.59
142-N120-FR	4.00	97.41	95.77	90.95	85.47	74.45	120.57	119.45	112.55	103.25	91.75
142-N120-FR	6.00	173.11	170.45	161.34	143.15	119.29	201.42	199.08	191.99	179.79	160.09
142-N150-FR	1.28	12.94	12.94	12.26	11.18	10.02	14.37	14.35	13.80	12.52	11.12
142-N150-FR	4.00	97.86	96.56	92.51	81.59	68.18	128.76	127.50	121.49	112.61	100.54
142-N150-FR	6.00	162.37	158.99	148.73	131.58	110.03	197.41	195.84	190.05	179.26	162.44
202-N100-FR	1.39	12.56	12.47	11.96	10.63	-	13.51	13.50	13.49	12.60	-
202-N100-FR	4.00	93.07	92.40	88.79	80.58	-	108.50	107.91	104.75	93.06	-
202-N100-FR	6.00	188.63	184.77	173.76	158.15	-	227.47	226.40	217.24	195.81	-
202-N120-FR	1.39	12.81	12.71	12.09	10.81	-	15.18	15.17	15.14	13.60	-
202-N120-FR	4.00	97.11	96.36	91.70	83.85	-	116.44	115.64	109.98	98.16	-
202-N120-FR	6.00	191.80	188.23	177.94	160.81	-	230.69	229.94	221.98	203.79	-
202-N150-FR	1.39	13.15	13.02	12.27	11.14	-	16.45	16.45	16.05	14.17	-
202-N150-FR	4.00	102.42	101.16	95.83	89.27	-	128.20	126.06	117.79	106.42	-
202-N150-FR	6.00	188.24	186.47	179.66	159.06	-	238.28	229.36	222.60	207.03	-
302-N100-FR	1.98	24.64	24.63	23.83	22.17	-	26.27	26.26	25.67	23.37	-
302-N100-FR	4.00	93.86	93.80	93.20	85.10	-	104.53	104.29	102.32	94.27	-
302-N100-FR	6.00	196.88	195.50	187.10	169.77	-	230.30	229.11	203.98	194.41	-
302-N120-FR	1.98	26.01	25.97	25.30	22.38	-	27.17	27.16	27.12	23.49	-
302-N120-FR	4.00	97.47	97.47	95.87	86.44	-	111.32	111.12	110.55	97.50	-
302-N120-FR	6.00	202.58	201.16	193.42	174.59	-	241.24	239.93	233.04	199.24	-
302-N150-FR	1.99	27.71	27.51	26.10	23.24	-	28.56	28.55	28.54	24.25	-
302-N150-FR	4.00	103.08	102.77	98.41	89.34	-	120.82	120.58	118.63	101.37	-
302-N150-FR	6.00	210.15	208.63	199.80	179.71	-	247.08	246.04	240.85	205.67	-

Table 3 Web crippling strengths of duplex stainless steel sections predicted from finite element analysis

B. *a*/*h* for offset circular web opening case

Specimen	Thickness	Unfastened FEA load per web, P_{FEA}				Fastened FEA load per web, P_{FEA}			
	t	A (0)	A (0.2)	A (0.4)	A (0.6)	A (0)	A (0.2)	A (0.4)	A (0.6)
	(mm)	(kN)	(kN)	(kN)	(kN)	(kN)	(kN)	(kN)	(kN)
142-N100-FR	1.27	11.50	11.46	11.27	10.95	12.73	12.71	12.63	12.53
142-N100-FR	4.00	93.24	93.15	92.67	91.75	112.63	112.62	112.55	112.49
142-N100-FR	6.00	166.59	166.08	164.37	160.39	201.87	201.39	199.44	186.56
142-N120-FR	1.27	12.19	12.11	11.90	11.41	13.45	13.44	13.43	13.38
142-N120-FR	4.00	97.47	97.33	96.72	95.53	120.57	120.57	120.47	120.24
142-N120-FR	6.00	166.56	166.09	164.36	159.70	201.42	200.93	198.95	186.40
142-N150-FR	1.28	12.97	12.87	12.53	11.88	14.39	14.38	14.34	14.27
142-N150-FR	4.00	97.77	97.39	96.13	93.66	128.76	128.73	128.48	125.80
142-N150-FR	6.00	158.21	157.58	155.68	152.08	197.41	196.97	195.04	184.86
202-N100-FR	1.39	12.36	12.07	11.44	10.37	14.27	14.27	14.17	14.03
202-N100-FR	4.00	93.01	92.74	91.86	90.03	108.50	108.47	108.37	108.25
202-N100-FR	6.00	184.32	183.61	181.12	175.45	227.47	226.95	224.65	212.61
202-N120-FR	1.39	12.61	12.35	11.65	10.51	14.34	14.34	14.24	14.06
202-N120-FR	4.00	97.07	96.78	95.72	93.16	116.44	116.41	116.30	116.13
202-N120-FR	6.00	185.87	185.13	182.63	176.05	230.69	229.99	227.02	213.26
202-N150-FR	1.39	12.95	12.67	11.93	10.90	16.45	16.44	16.30	16.05
202-N150-FR	4.00	102.38	101.94	100.36	95.45	127.48	127.41	127.27	126.92
202-N150-FR	6.00	187.98	187.16	184.31	176.30	229.87	229.12	225.97	212.56
302-N100-FR	1.98	22.75	22.66	22.29	21.36	26.27	26.26	26.15	25.72
302-N100-FR	2.00	93.88	93.48	91.97	88.40	104.53	104.52	104.46	104.31
302-N100-FR	4.00	194.66	193.59	189.95	178.72	230.30	230.06	228.73	212.81
302-N120-FR	1.98	24.06	23.91	23.10	21.95	27.17	27.15	26.96	26.57
302-N120-FR	2.00	97.50	96.93	95.23	90.39	111.36	111.35	111.21	111.02
302-N120-FR	4.00	197.85	196.83	192.58	176.63	241.24	240.59	237.63	226.42
302-N150-FR	1.99	25.42	25.08	24.17	22.58	28.56	28.53	28.38	27.19
302-N150-FR	2.00	103.09	102.44	100.01	93.97	120.82	120.80	120.74	120.02
302-N150-FR	4.00	202.77	201.35	195.45	184.86	247.08	246.05	241.93	227.42

Table 3 Web crippling strengths of duplex stainless steel sections predicted from finite element analysis

C. *x*/*h* for offset circular web opening case

Specimen	Thickness	Unfastened FEA load per web, P_{FEA}				Fastened FEA load per web, P_{FEA}			
	t	*A* (0)	*A* (0.2)	*A* (0.4)	*A* (0.6)	*A* (0)	*A* (0.2)	*A* (0.4)	*A* (0.6)
	(mm)	(kN)	(kN)	(kN)	(kN)	(kN)	(kN)	(kN)	(kN)
142-N100-A0-FR	1.27	11.13	11.13	11.13	11.13	12.12	12.12	12.12	12.12
142-N100-A0.2-FR	1.27	10.99	10.99	11.00	11.03	12.04	12.05	12.06	12.08
142-N100-A0.4-FR	1.27	10.50	10.54	10.64	10.79	11.75	11.80	11.87	11.99
142-N100-A0.6-FR	1.27	9.56	9.80	10.12	10.44	11.09	11.26	11.60	11.88
142-N100-A0.8-FR	1.27	8.15	8.76	9.21	9.60	---	---	---	---
142-N120-A0-FR	1.27	11.88	11.88	11.88	11.88	12.99	12.99	12.99	12.99
142-N120-A0.2-FR	1.27	11.70	11.71	11.72	11.76	12.91	12.92	12.93	12.96
142-N120-A0.4-FR	1.27	11.07	11.09	11.26	11.45	12.56	12.56	12.73	12.88
142-N120-A0.6-FR	1.27	9.85	10.16	10.52	10.86	11.66	11.95	12.40	12.74
142-N120-A0.8-FR	1.27	8.43	9.05	9.53	9.85	9.55	10.74	11.64	12.38
142-N150-A0-FR	1.28	12.75	12.75	12.75	12.75	14.42	14.42	14.42	14.42
142-N150-A0.2-FR	1.28	12.56	12.58	12.60	12.62	13.87	13.90	13.91	14.34
142-N150-A0.4-FR	1.28	11.64	11.70	11.91	12.31	13.35	13.40	13.62	13.81
142-N150-A0.6-FR	1.28	10.35	10.68	11.04	11.37	12.26	12.66	13.16	13.58
142-N150-A0.8-FR	1.28	8.96	9.53	9.98	10.27	10.29	11.36	12.21	12.98
202-N100-A0-FR	1.39	12.40	12.40	12.40	12.40	13.50	13.50	13.50	13.50
202-N100-A0.2-FR	1.39	12.10	12.11	12.12	12.14	13.39	13.40	13.41	13.47
202-N100-A0.4-FR	1.39	10.98	11.06	11.21	11.41	12.26	12.27	12.44	12.67
202-N100-A0.6-FR	1.39	9.46	9.76	10.08	10.36	11.28	11.53	11.98	12.44
202-N120-A0-FR	1.39	12.69	12.69	12.69	12.69	15.16	15.16	15.16	15.16
202-N120-A0.2-FR	1.39	12.35	12.37	12.38	12.39	15.05	15.05	15.07	15.14
202-N120-A0.4-FR	1.39	11.19	11.41	11.44	11.63	14.30	14.35	14.63	14.90
202-N120-A0.6-FR	1.39	9.66	9.96	10.26	10.53	13.00	13.38	13.95	14.54
202-N150-A0-FR	1.45	14.28	14.28	14.28	14.28	16.45	16.45	16.45	16.45
202-N150-A0.2-FR	1.45	13.87	13.88	13.89	13.94	16.26	16.27	16.30	16.38
202-N150-A0.4-FR	1.45	12.61	12.71	12.88	13.06	15.28	15.38	15.71	16.04
202-N150-A0.6-FR	1.45	11.00	11.30	11.60	11.85	13.78	14.23	14.87	15.52
302-N100-A0-FR	1.98	24.25	24.25	24.25	24.25	25.62	25.62	25.62	25.62
302-N100-A0.2-FR	1.98	24.00	24.01	24.03	24.09	26.55	26.56	25.60	25.58
302-N120-A0-FR	1.96	25.23	25.23	25.23	25.23	26.63	26.63	26.63	26.63
302-N120-A0.2-FR	1.96	24.80	24.83	24.86	24.94	26.51	26.53	26.62	26.59
302-N120-A0.4-FR	1.96	22.74	22.87	23.29	23.79	24.46	24.66	25.34	25.45

Table 3 Web crippling strengths of duplex stainless steel sections predicted from finite element analysis

C. Continued

Specimen	Thickness	Unfastened FEA load per web, P_{FEA}				Fastened FEA load per web, P_{FEA}			
	t	A (0)	A (0.2)	A (0.4)	A (0.6)	A (0)	A (0.2)	A (0.4)	A (0.6)
	(mm)	(kN)	(kN)	(kN)	(kN)	(kN)	(kN)	(kN)	(kN)
302-N120-A0.6-FR	1.96	18.80	20.00	21.35	23.24	23.25	23.30	24.50	24.59
302-N150-A0-FR	1.99	27.55	27.55	27.55	27.55	28.10	28.10	28.10	28.10
302-N150-A0.2-FR	1.99	26.79	26.83	26.87	27.02	27.93	28.02	28.10	28.41
302-N150-A0.4-FR	1.99	24.26	24.40	24.87	25.44	26.90	27.25	27.63	27.83
302-N150-A0.6-FR	1.99	20.84	21.56	22.58	23.74	23.84	24.86	26.59	26.70

Table 4 Coefficients of the proposed strength reduction factor equations

	Stainless steel grade	Coefficient	Unfastened to bearing plate	Fastened to bearing plate
Strength reduction factor Eqs. (17) and (18)	EN 1.4462 (Duplex)	α	1.11	1.08
		γ	0.37	0.33
		λ	0.04	0.01
		ρ	0.91	0.89
		μ	0.19	0.24
		ζ	0.11	0.11
	EN 1.4404 (Austenitic)	α	1.12	1.08
		γ	0.29	0.28
		λ	0.08	0.02
		ρ	0.91	0.95
		μ	0.20	0.13
		ζ	0.11	0.07
	EN 1.4003 (Ferritic)	α	1.15	1.1
		γ	0.36	0.28
		λ	0.10	0.05
		ρ	0.91	0.92
		μ	0.20	0.20
		ζ	0.11	0.07

the three stainless steel grades: duplex EN1.4462, austenitic EN1.4404 and ferretic EN1.4003. Table 3 shows the web crippling strengths determined from finite element analyses for the duplex grade EN 1.4462. Similar web crippling strengths were also determined for the austenitic grade 1.4404 and ferritic grade 1.4003. The web crippling strengths for sections with circular web openings were divided by that for sections without web openings and considered as the strength reduction factor (R).

Fig. 7(a) shows the ratio of the circular web opening depth to the flat portion of the web (*a*/*h*) versus the strength reduction factor, for the three stainless steel grades. As can be seen, the reduction in strength increases as the parameter *a*/*h* increases for all three stainless steels, inparticular for the ferritic grade. The reduction in strength of the ferritic grade 6 mm thick section is smallest and the reduction in strength increases as the section becomes thinner. It can be seen that when the *a*/*h* ratio increases from 0.2 to 0.8, the reduction in strength for the ferritic grade increases by 36%. From Fig. 7(b) it can be seen that the reduction in strength is sensitive to the horizontal distance of the web openings to the bearing plate. As the ratio of *x*/*h* decreases from 0.6 to 0.2, the strength reduction factor decreases by 7%. Also, it can again be seen that the reduction in strength is less for the austenitic grade compared to that of the other two stainless steel grades.

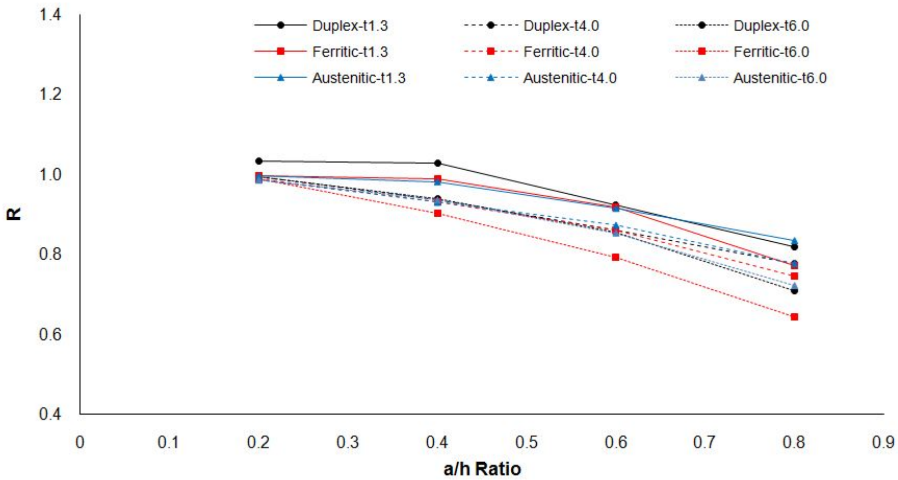

(a) With *a*/*h* for centered circular web opening

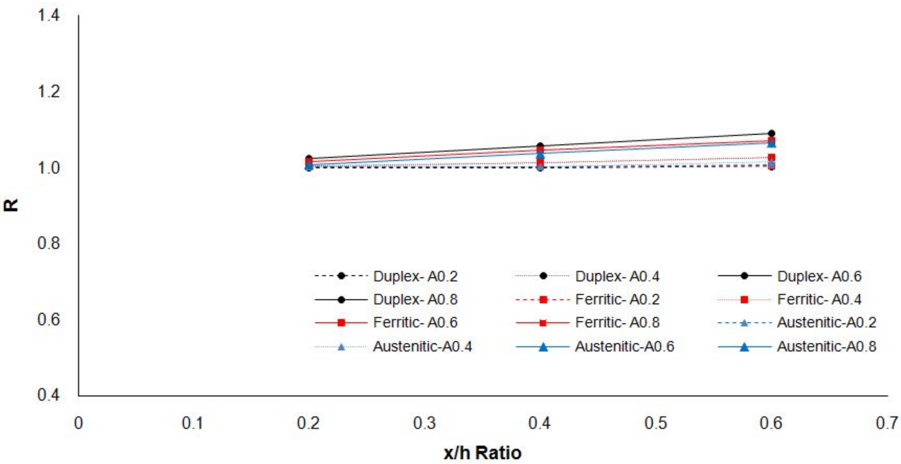

(b) With *x*/*h* for offset circular web opening

Fig. 7 Variation in reduction factors for C142 section for the case of flange unfastened to bearing plate

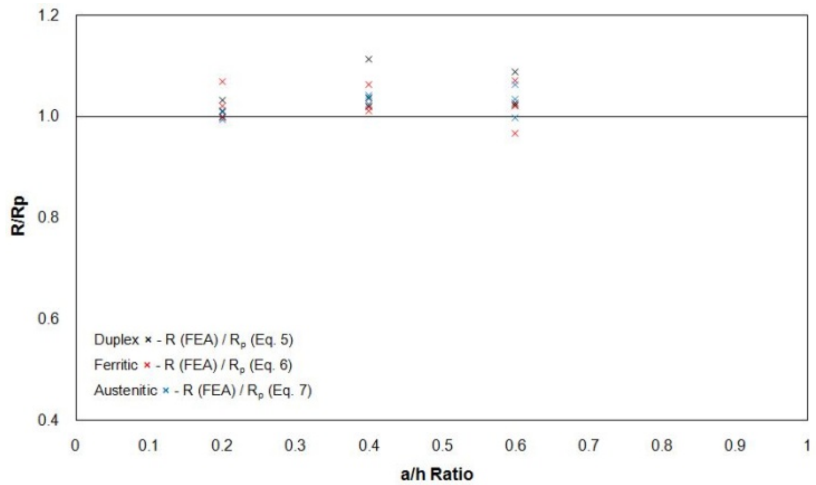

(a) With centered circular web opening

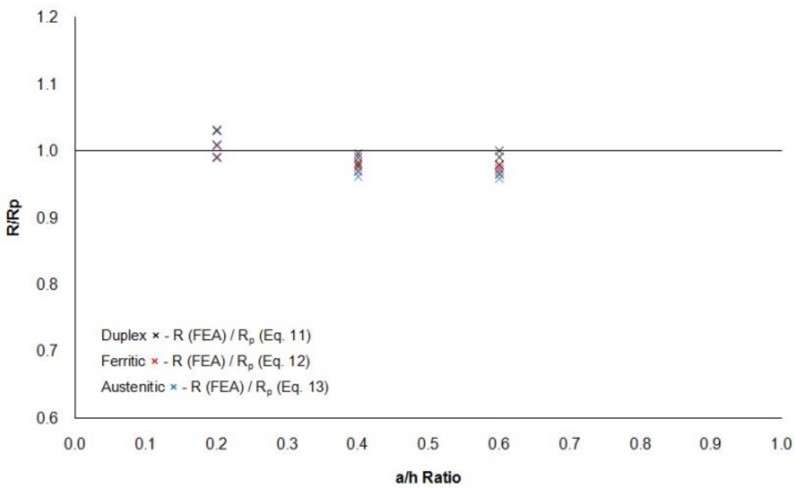

(b) With offset circular web opening

Fig. 8 Comparison of strength reduction factor for C142 section for the case of flange unfastened to bearing plate

4. Reduction factor comparison with Lian (Lian *et al.* 2016a, b, Lian 2016)

For ease of reference, the reduction factor equations proposed by Lian (Lian *et al*. 2016a, b, Lian 2016) are summarised below:

For centered web opening:

Free case $$R_P = 0.98 - 0.26(\frac{a}{h}) + 0.06(\frac{N}{h}) \quad (1)$$

Fixed case $$R_P = 0.95 - 0.06(\frac{a}{h}) + 0.01(\frac{N}{h}) \quad (2)$$

For offset web opening:

Free case $$R_P = 0.99 - 0.26(\frac{a}{h}) + 0.11(\frac{x}{h}) \quad (3)$$

Fixed case $$R_P = 0.99 - 0.14(\frac{a}{h}) + 0.07(\frac{x}{h}) \quad (4)$$

where the limits for the reduction factor in Eqs. (1)-(4) are $h/t \le 157.8$, $N/t \le 120.97$, $N/h \le 1.15$, $a/h \le 0.8$, and $\theta = 90°$.

In order to evaluate the applicability of the proposed equations to cold-formed stainless steel grades, an extensive statistical analysis was performed on all four proposed equations. Table 5 compares the reduction factors determined from the finite element models to Eqs. (1)-(4) for cases of centred and offset web opening where the flange is unfastened to the bearing plate.

As can be seen from Table 5, the four equations proposed by Lian (Lian *et al*. 2016a, b, Lian 2016) for carbon steel are conservative for the three stainless steel grades, especially for sections with centred web openings. Examining the strength reduction factor ratios obtained from the finite element analyses, with the exception of the offset web opening fixed case which has a mean reduction factor ratio of 0.99 and coefficient of variation (COV) of 0.05, the other reduction factors from Lian (Lian *et al*. 2016a, b, Lian 2016) are conservative for the stainless steel grades, especially for the ferritic and austenitic stainless steel grades. For example, for the centred web opening case for austenitic grade, the mean value of the web crippling reduction factor ratio is 1.09 and 1.07 for the cases of flange unfastened and fastened to the bearing plate, respectively; the corresponding values of COV are 0.04 and 0.01, respectively. In the next section, new equations are proposed for each of the three stainless steel grades.

Table 5 Comparison of web crippling strength reduction factor for cold-formed stainless steel lipped channel-sections with reduction factors equations proposed by Lian (Lian *et al*. 2016a, b, Lian 2016)

A. Flange unfastened to the bearing plate

Specimen	Factored resistance (Eq. (1))	Factored resistance (Eq. (3))	Reduction factor						Comparison with resistance from Lian, R / R_{Lian}					
			Duplex		Ferritic		Austenitic		Duplex		Ferritic		Austenitic	
			$R = P(Opening) / P(A0)$											
	Centred	Offset	Centred	Offset	Centred	Offset	Centred	Offset	Centred	Offset	Centred	Offset	Centred	Offset
142-N100-MA0.6-FR	0.86	0.90	0.89	0.90	0.93	0.93	0.91	0.91	1.04	1.01	1.07	1.04	1.06	1.01
142-N120-MA0.6-FR	0.87	0.90	0.87	0.89	0.91	0.92	0.92	0.92	1.00	0.99	1.04	1.03	1.05	1.03
142-N150-MA0.4-FR	0.94	0.93	0.94	0.87	0.95	0.96	0.96	0.94	1.00	0.94	1.02	1.04	1.03	1.01
202-N100-MA0.4-FR	0.90	0.93	0.95	0.90	0.99	0.94	0.99	0.94	1.05	0.97	1.10	1.02	1.10	1.02
202-N100-MA0.6-FR	0.85	0.90	0.84	0.81	0.90	0.90	0.94	0.93	0.99	0.91	1.05	1.01	1.11	1.03
202-N120-MA0.4-FR	0.91	0.93	0.94	0.90	0.97	0.93	0.99	0.95	1.03	0.97	1.06	1.00	1.09	1.03
202-N120-MA0.6-FR	0.86	0.90	0.84	0.83	0.86	0.87	0.91	0.93	0.98	0.93	1.01	0.97	1.07	1.04
202-N150-MA0.4-FR	0.92	0.93	0.93	0.99	0.94	0.99	0.97	1.03	1.01	1.07	1.02	1.07	1.06	1.11
302-N100-MA0.6-FR	0.84	0.90	0.89	0.95	0.98	0.99	0.98	1.04	1.07	1.06	1.17	1.11	1.17	1.16
302-N120-MA0.6-FR	0.84	0.90	0.86	0.96	0.93	1.00	0.98	1.08	1.01	1.07	1.10	1.11	1.16	1.20
302-N150-MA0.6-FR	0.85	0.90	0.83	0.93	0.89	1.00	0.94	1.04	0.98	1.04	1.04	1.11	1.10	1.16
Mean, P_m									1.02	1.00	1.06	1.05	1.09	1.07
Coefficient of variation, V_p									0.03	0.06	0.04	0.05	0.04	0.07

Table 5 Comparison of web crippling strength reduction factor for cold-formed stainless steel lipped channel-sections with reduction factors equations proposed by Lian (Lian *et al*. 2016a, b, Lian 2016)

B. Flange fastened to the bearing plate

Specimen	Factored resistance (Eq. (1))	Factored resistance (Eq. (3))	Reduction factor $R = P(Opening) / P(A0)$						Comparison with resistance from Lian, R / R_{Lian}					
			Duplex		Ferritic		Austenitic		Duplex		Ferritic		Austenitic	
	Centred	Offset	Centred	Offset	Centred	Offset	Centred	Offset	Centred	Offset	Centred	Offset	Centred	Offset
142-N100-MA0.6-FX	0.92	0.94	0.98	0.93	0.99	0.94	0.98	0.92	1.07	0.98	1.08	1.00	1.07	0.97
142-N120-MA0.6-FX	0.92	0.94	0.99	0.94	0.99	0.94	0.98	0.93	1.08	1.00	1.08	1.00	1.07	0.99
142-N150-MA0.4-FX	0.93	0.96	0.99	0.94	0.99	0.95	0.99	0.95	1.06	0.98	1.06	0.99	1.06	0.99
202-N100-MA0.4-FX	0.93	0.96	0.99	0.87	0.99	0.86	0.98	0.85	1.07	0.91	1.07	0.90	1.06	0.89
202-N100-MA0.6-FX	0.91	0.94	0.98	0.83	0.99	0.86	0.97	0.85	1.07	0.89	1.08	0.91	1.06	0.90
202-N120-MA0.4-FX	0.93	0.96	0.99	1.02	0.99	1.00	0.99	1.00	1.07	1.06	1.07	1.04	1.06	1.04
202-N120-MA0.6-FX	0.92	0.94	0.98	1.01	0.98	1.00	0.98	1.00	1.07	1.07	1.07	1.06	1.07	1.06
202-N150-MA0.4-FX	0.93	0.96	0.99	0.95	0.99	0.95	0.99	0.96	1.06	0.99	1.07	0.99	1.06	1.01
302-N100-MA0.6-FX	0.91	0.94	0.97	0.99	0.99	0.95	0.98	0.96	1.07	1.05	1.08	1.01	1.08	1.02
302-N120-MA0.6-FX	0.91	0.94	0.97	0.90	0.99	0.92	0.99	0.92	1.07	0.95	1.08	0.98	1.08	0.98
302-N150-MA0.6-FX	0.91	0.94	0.95	0.93	0.99	0.94	0.97	0.96	1.04	0.99	1.08	1.00	1.06	1.01
Mean, P_m									1.06	0.99	1.07	0.99	1.07	0.99
Coefficient of variation, V_p									0.01	0.06	0.01	0.05	0.01	0.05

5. Proposed strength reduction factors

Table 3 shows the dimensions considered and web crippling strengths of the duplex grade stainless steel sections predicted from the finite element analysis. (Tables for the austenitic and ferritic stainless steel grades can be found in Appendices A and B). Using bivariate linear regression analysis, two unified strength reduction factor equations (R_p) for three stainless steel grades with web openings are proposed. The equations are as follows

Centred web opening $$R_p = \alpha - \gamma(\frac{a}{h}) - \lambda(\frac{N}{h}) \leq 1 \quad (5)$$

Offset web opening $$R_p = \rho + \mu(\frac{a}{h}) + \zeta(\frac{x}{h}) \leq 1 \quad (6)$$

The limits for the reduction factor Eqs. (5)-(6) remain $h/t \leq 157.8$, $N/t \leq 120.97$, $N/h \leq 1.15$, $a/h \leq 0.8$, and $\theta = 90°$. The coefficients α, γ, λ, ρ, μ and ζ of the equations are calibrated with the stainless steel analysis results, and the coefficients are presented in Table 4.

6. Comparison of numerical results with proposed reduction factors

For the three stainless steels grades, the values of the strength reduction factor (R) obtained from the numerical results are compared with the values of the proposed strength reduction factor (R_p) calculated using Eqs. (5)-(6). The results for C142 are shown in Fig. 8. In order to evaluate the accuracy of proposed equations, extensive statistical reliability analyses are performed. The results are summarized in Table 6. It should be noted, in calculating the reliability index, the resistance factor of ϕ = was used, corresponding to the reliability index β from the NAS specification. According to the NAS specification, design rules are reliable if the reliability index are more than 2.5. As can be seen in Table 6, the proposed reduction factors are a good match with the numerical results for the both cases of flanges unfastened and flanges fastened to the bearing plates and particularly for the duplex stainless steel grade.

Table 6 Statistical analysis of strength reduction factor

A. Duplex stainless steel grade

Statistical parameters	Centred circular web opening $R_{(FEA)} / R_p$		Offset circular web opening $R_{(FEA)} / R_p$	
	Unfastened to bearing plate	Fastened to bearing plate	Unfastened to bearing plate	Fastened to bearing plate
Number of data	90	90	84	81
Mean, P_m	1.00	1.01	1.04	1.04
Coefficient of variation, V_p	0.03	0.03	0.04	0.05
Reliability index, β	2.82	2.86	2.97	2.94
Resistance factor, ϕ	0.85	0.85	0.85	0.85

Table 6 Statistical analysis of strength reduction factor

B. Austenitic stainless steel grade

Statistical parameters	Centred circular web opening $R_{(FEA)}$ / R_p		Offset circular web opening $R_{(FEA)}$ / R_p	
	Unfastened to bearing plate	Fastened to bearing plate	Unfastened to bearing plate	Fastened to bearing plate
Number of data	90	90	84	81
Mean, P_m	0.99	0.99	1.00	1.01
Coefficient of variation, V_p	0.05	0.03	0.03	0.03
Reliability index, β	2.74	2.78	2.82	2.86
Resistance factor, ϕ	0.85	0.85	0.85	0.85

Table 6 Statistical analysis of strength reduction factor

C. Ferritic stainless steel grade

Statistical parameters	Centred circular web opening $R_{(FEA)}$ / R_p		Offset circular web opening $R_{(FEA)}$ / R_p	
	Unfastened to bearing plate	Fastened to bearing plate	Unfastened to bearing plate	Fastened to bearing plate
Number of data	90	90	84	81
Mean, P_m	1.00	0.99	1.00	1.0
Coefficient of variation, V_p	0.05	0.03	0.02	0.03
Reliability index, β	2.78	2.78	2.83	2.82
Resistance factor, ϕ	0.85	0.85	0.85	0.85

For example, for the centred circular web opening, the mean value of the web crippling reduction factor ratios are 1.00 and 1.01 for the cases of flange unfastened and flange fastened to the bearing plate, respectively. The corresponding values of COV are 0.03 and 0.03, respectively. Similarly, the reliability index values (β) are 2.82 and 2.86, respectively. For the offset circular web opening, the mean value of the web crippling reduction factor ratios are 1.04 and 1.04 for the cases of flange unfastened and flange fastened to the bearing plate, respectively. The corresponding values of COV are 0.04 and 0.05, respectively. Similarly, the reliability index values (β) are 2.97 and 2.94, respectively. Therefore, the proposed strength reduction factor equations are able to reliably predict the influence of the circular web openings on the web crippling strengths of cold-formed stainless steel lipped channel-sections under the interior-one-flange (IOF) loading condition.

7. Conclusions

In this study, the effect of circular web openings on the web crippling strength of cold-formed stainless steel lipped channel-sections was investigated. For this purpose, a parametric study of 2218 lipped channel-sections with various dimensions and thicknesses were considered for the three stainless steel grades: duplex EN1.4462, austenitic EN1.4404 and ferretic EN1.4003. Cases with and without circular web openings subjected to the interior-one-flange (IOF) loading condition were considered with web openings located centred beneath the bearing plate or with a horizontal clear distance to the near edge of the bearing plate.

In order to take into account the influence of the circular web openings, strength reduction factor equations were determined. Then, the strength reduction factor equations were compared to recent equations proposed for cold-formed carbon steel. It was observed that the cold-formed carbon steel strength reduction factors are conservative to the duplex grade by around 2% conservative to the austenitic and ferritic grades by around 9%.

New web crippling strength reduction factor equations were proposed for the both cases of flanges unfastened and flanges fastened to the bearing plates.In order to evaluate the reliability of proposed reduction factors, reliability analysis was performed. It was demonstrated that the proposed strength reduction factors are generally conservative and agree well with the analysis results. The proposed new strength reduction factors have the capability to produce safe yet not too conservative design values when calibrated with the resistance factor of 0.85 (φ = 0.85) according to the NAS specification.

References

ABAQUS (2014), Analysis User's Manual-Version 6.14-2 ABAQUS Inc., USA.

Arrayago, I., Real, E. and Gardner, L. (2015), "Description of stress–strain curves for stainless steel alloys", *Mater. Des.*, **87**, 540-552.

AS/NZS 4600 (2005), Cold-formed steel structures: AS/NZS 4600:2005, Standards Australia, Sydney, Australia.

ASCE 8-02 (2002), Specification for the Design of Cold-Formed Stainless Steel Structural Members, SEI/ASCE 8-02, Reston, VA, USA.

Chen, J. and Young, B. (2006), "Stress-strain curves for stainless steel at elevated temperatures", *Eng. Struct.*, **28**(2), 229-239.

Dai, X. and Lam, D. (2010), "Axial compressive behaviour of stub concrete-filled columns with elliptical stainless steel hollow sections", *Steel Compos. Struct., Int. J.*, **10**(6), 517-539.

Kiymaz, G. and Seckin, E. (2014), "Behavior and design of stainless steel tubular member welded end connections", *Steel Compos. Struct., Int. J.*, **17**(3), 253-269.

Korvink, S.A., van den Berg, G.J. and van der Merwe, P. (1995), "Web crippling of stainless steel cold-formed beams", *J. Construct. Steel Res.*, **34**(2-3), 225-248.

Lawson, R.M., Basta, A. and Uzzaman, A. (2015), "Design of stainless steel sections with circular openings in shear", *J. Construct. Steel Res.*, **112**, 228-241.

Lian, Y. (2016), "Web crippling behaviour of cold-formed steel sections with circular web openings under one-flange loading", Ph.D. Thesis; School of Planning, Architecture and Civil Engineering, The Queen's University of Belfast, Northern Ireland, UK.

Lian, Y., Uzzaman, A., Lim, J.B.P., Abdelal, G., Sha, W., Nash, D. and Young, B. (2016a), "Experimental and numerical investigation of cold-formed steel sections with web openings under one-flange loading condition subjected to web crippling", *Proceeding of the 8th International Conference on Steel and Aluminium Structures*, Hong Kong, December.

Lian, Y., Uzzaman, A., Lim, J.B.P., Abdelal, G., Sha, W., Nash, D. and Young, B. (2016b), "Parametric studies and design recommendations of cold-formed steel sections with web openings under one-flange loading condition subjected to web crippling", *Proceeding of The 8th International Conference on Steel and Aluminium Structures*, Hong Kong, December.

Lian, Y., Uzzaman, A., Lim, J.B.P., Abdelal, G., Nash, D. and Young, B. (2016c), "Effect of web holes on web crippling strength of cold-formed steel channel sections under end-one-flange loading condition - Part I: Tests and finite element analysis", *Thin-Wall*. *Struct*. [Under Review]

Lian, Y., Uzzaman, A., Lim, J.B.P., Abdelal, G., Nash, D. and Young, B. (2016d), "Effect of web holes on web crippling strength of cold-formed steel channel sections under end-one-flange loading condition - Part II: Parametric study and proposed design equations", *Thin-Wall*. *Struct*. [Under Review]

Lim, J.B.P. and Nethercot, D.A. (2001), "Ultimate strength of bolted moment-connections between cold-formed steel members", *Thin-Wall*. *Struct*., **41**(11), 1019-1039.

NAS (2007), North American Specification for the Design of Cold-Formed Steel Structural Members: American Iron and Steel Institute, AISI S100-2007, AISI Standard.

Natário, P., Silvestre, N. and Camotim, D. (2016), "Direct strength prediction of web crippling failure of beams under ETF loading", *Thin-Wall*. *Struct*., **98(**B), 360-374.

Rezvani, F.H., Yousefi, A.M. and Ronagh, H.R. (2015), "Effect of span length on progressive collapse behaviour of steel moment resisting frames", *Structures*, **3**, 81-89.

Sundararajah, L., Mahendran, M. and Keerthan, P. (2016), "Experimental studies of lipped channel beams subject to web crippling under two-flange load cases", *J. Struct*. *Eng*.

Theofanous, M. and Gardner, L. (2012), "Effect of element interaction and material nonlinearity on the ultimate capacity of stainless steel cross-sections", S*teel Compos*. *Struct*., *Int*. *J*., **12**(1), 73-92.

Uzzaman, A., Lim, J.B.P., Nash, D., Rhodes, J. and Young, B. (2012a), "Web crippling behaviour of cold-formed steel channel sections with offset web holes subjected to interior-two-flange loading", *Thin-Wall*. *Struct*., **50**(1), 76-86.

Uzzaman, A., Lim, J.B.P., Nash, D., Rhodes, J. and Young, B. (2012b), "Cold-formed steel sections with web openings subjected to web crippling under two-flange loading conditions-part I: Tests and finite element analysis", *Thin-Wall*. *Struct*., **56**, 38-48.

Uzzaman, A., Lim, J.B.P., Nash, D., Rhodes, J. and Young, B. (2012c), "Cold-formed steel sections with web openings subjected to web crippling under two-flange loading conditions-part II: Parametric study and proposed design equations", *Thin-Wall*. *Struct*.*s*, **56**, 79-87.

Uzzaman, A., Lim, J.B.P., Nash, D., Rhodes, J. and Young, B. (2013), "Effect of offset web holes on web crippling strength of cold-formed steel channel sections under end-two-flange loading condition", *Thin-Wall*. *Struct*., **65**, 34-48.

Yousefi, A.M., Hosseini, M. and Fanaie, N. (2014), "Vulnerability assessment of progressive collapse of steel moment resistant frames", *Trend*. *Appl*. *Sci*. *Res*., **9**(8), 450-460.

Zhou, F. and Young, B. (2006), "Yield line mechanism analysis on web crippling of cold-formed stainless steel tubular sections under two-flange loading", *Eng*. *Struct*., **28**(6), 880-892.

Zhou, F. and Young, B. (2007), "Cold-formed high-strength stainless steel tubular sections subjected to web crippling", *J*. *Struct*. *Eng*., **133**(3), 368-377.

Zhou, F. and Young, B. (2013), "Web crippling behaviour of cold-formed duplex stainless steel tubular sections at elevated temperatures", *Eng*. *Struct*., **57**, 51-62.

BU

Nomenclature

A	Web opening ratio;
a	Diameter of circular web opening;
b_f	Overall flange width of section;
b_l	Overall lip width of section;
COV	Coefficient of variation;
d	Overall web depth of section;
E	Young's modulus of elasticity;
h	Depth of the flat portion of web;
L	Length of the specimen;
N	Length of the bearing plate;
P_{ASCE}	Nominal web crippling strength obtained from American Code;
$P_{\mathrm{AS/NZS}}$	Nominal web crippling strength obtained from Australian/New Zealand Code;
P_{FEA}	Web crippling strength per web predicted from finite element (FEA);
P_{NAS}	Nominal web crippling strength obtained from North American Specification;
P_m	Mean value of analysed-to-predicted load ratio;
R	Reduction factor;
R_P	Proposed reduction factor;
r_i	Inside corner radius of section;
θ	Angle between web and bearing surface
t	Thickness of section;
V_P	Coefficient of variation of Analysed-to-predicted load ratio;
x	Horizontal clear distance of the web openings to the near edge of the bearing plate;
β	Reliability index;

Appendix A: Austenitic

Table A Web crippling strengths of austenitic stainless steel sections predicted from finite element analysis (a) *a/h* for centred circular web opening case

Specimen	Thickness	Unfastened FEA load per web, P_{FEA}					Fastened FEA load per web, P_{FEA}				
	t	*A* (0)	*A* (0.2)	*A* (0.4)	*A* (0.6)	*A* (0.8)	*A* (0)	*A* (0.2)	*A* (0.4)	*A* (0.6)	*A* (0.8)
	(mm)	(kN)	(kN)	(kN)	(kN)	(kN)	(kN)	(kN)	(kN)	(kN)	(kN)
142-N100-FR	1.27	9.64	9.55	9.50	8.98	7.98	10.13	10.01	9.83	9.57	8.56
142-N100-FR	4.00	75.39	74.54	70.34	64.89	56.30	86.65	86.32	83.06	78.31	70.35
142-N100-FR	6.00	137.93	136.61	124.50	109.57	88.79	170.00	167.14	158.77	145.91	135.41
142-N120-FR	1.27	10.30	10.25	10.23	9.38	8.37	11.01	10.99	10.88	10.17	9.03
142-N120-FR	4.00	78.92	77.99	73.93	67.87	56.96	94.74	94.16	89.69	82.18	73.45
142-N120-FR	6.00	138.00	134.32	124.67	108.57	87.95	172.45	168.87	160.43	148.22	130.58
142-N150-FR	1.28	11.15	11.12	10.69	9.77	8.80	11.91	11.94	11.64	10.72	9.62
142-N150-FR	4.00	79.09	78.31	74.62	66.02	53.18	102.89	101.57	101.57	90.09	80.21
142-N150-FR	6.00	132.05	129.07	120.00	103.68	82.86	170.58	167.70	160.53	149.33	133.15
202-N100-FR	1.39	10.95	10.93	10.92	9.86	-	10.99	10.97	10.56	10.47	-
202-N100-FR	4.00	76.67	76.06	73.11	66.17	-	84.44	84.09	82.29	75.25	-
202-N100-FR	6.00	153.20	150.53	142.09	128.00	-	179.07	177.81	172.61	155.54	-
202-N120-FR	1.39	11.59	11.58	11.25	10.05	-	12.51	12.37	12.24	11.90	-
202-N120-FR	4.00	80.57	79.82	75.72	69.10	-	92.59	92.32	88.81	79.69	-
202-N120-FR	6.00	158.38	157.84	146.08	129.79	-	194.15	192.76	184.90	166.88	-
202-N150-FR	1.39	12.25	12.18	11.52	10.38	-	13.73	13.46	13.14	12.49	-
202-N150-FR	4.00	85.51	84.46	79.56	73.90	-	104.08	102.52	96.97	88.13	-
202-N150-FR	6.00	161.20	158.91	149.02	128.86	-	213.37	204.50	193.90	175.41	-
302-N100-FR	1.98	20.65	20.60	20.55	20.41	-	20.91	20.89	20.26	19.91	-
302-N100-FR	4.00	77.78	77.71	76.25	72.26	-	80.76	80.64	78.58	75.58	-
302-N100-FR	6.00	163.56	162.23	159.46	141.16	-	175.68	175.16	169.02	159.23	-
302-N120-FR	1.98	22.47	22.24	22.16	21.04	-	21.96	21.95	21.80	20.62	-
302-N120-FR	4.00	82.48	82.46	81.75	74.75	-	87.93	87.73	86.99	79.95	-
302-N120-FR	6.00	171.22	169.60	163.26	146.01	-	192.12	191.29	187.23	166.10	-
302-N150-FR	1.99	24.65	24.55	24.47	22.01	-	23.59	23.57	23.26	21.28	-
302-N150-FR	4.00	88.92	88.82	86.90	78.24	-	97.97	97.61	95.84	84.30	-
302-N150-FR	6.00	181.23	179.42	170.46	154.64	-	215.29	213.67	205.54	174.956	-

Table A Web crippling strengths of austenitic stainless steel sections predicted from finite element analysis
(b) *a/h* for offset circular web opening case

Specimen	Thickness	Unfastened FEA load per web, P_{FEA}				Fastened FEA load per web, P_{FEA}			
	t	A (0)	A (0.2)	A (0.4)	A (0.6)	A (0)	A (0.2)	A (0.4)	A (0.6)
	(mm)	(kN)	(kN)	(kN)	(kN)	(kN)	(kN)	(kN)	(kN)
142-N100-FR	1.27	8.47	8.44	8.27	8.14	9.40	9.37	9.32	9.24
142-N100-FR	4.00	66.60	66.54	66.20	65.49	80.85	80.83	80.78	80.74
142-N100-FR	6.00	121.33	120.59	118.39	114.61	155.17	154.74	153.12	142.44
142-N120-FR	1.27	8.89	8.88	8.80	8.66	9.90	9.86	9.82	9.76
142-N120-FR	4.00	69.52	69.40	68.93	67.89	86.20	86.18	86.11	85.83
142-N120-FR	6.00	120.01	119.35	117.73	114.98	155.65	155.18	153.51	142.84
142-N150-FR	1.28	9.61	9.59	9.48	9.32	10.52	10.50	10.47	10.45
142-N150-FR	4.00	69.82	69.41	68.27	66.25	91.06	91.02	90.85	90.16
142-N150-FR	6.00	114.61	113.88	112.10	109.53	152.49	152.09	150.57	142.00
202-N100-FR	1.39	9.43	9.35	7.95	7.76	10.63	10.60	10.51	10.38
202-N100-FR	4.00	67.75	67.60	67.13	66.11	78.80	78.76	78.72	78.69
202-N100-FR	6.00	136.09	135.62	133.92	128.96	167.89	167.88	167.76	166.51
202-N120-FR	1.39	9.95	9.89	9.71	9.48	10.60	10.57	10.51	10.39
202-N120-FR	4.00	70.69	70.46	69.91	68.69	84.52	84.50	84.49	84.44
202-N120-FR	6.00	137.96	137.13	134.60	130.87	177.96	177.92	177.66	169.46
202-N150-FR	1.39	10.74	10.68	10.49	10.10	12.16	12.14	12.09	12.01
202-N150-FR	4.00	74.59	74.40	73.69	72.19	92.62	92.61	92.57	92.41
202-N150-FR	6.00	139.46	138.88	137.06	132.55	185.28	184.93	183.42	170.70
302-N100-FR	1.98	17.02	16.94	16.80	16.64	19.25	19.23	19.16	19.05
302-N100-FR	2.00	69.18	69.08	68.69	67.88	76.40	76.35	76.30	76.22
302-N100-FR	4.00	146.80	146.49	145.30	141.51	168.78	168.74	168.72	168.65
302-N120-FR	1.98	17.95	17.92	17.84	17.66	19.80	19.77	19.72	19.66
302-N120-FR	2.00	72.56	72.47	71.98	71.03	81.28	81.25	81.19	81.09
302-N120-FR	4.00	151.85	151.49	149.92	143.33	179.93	179.90	179.87	179.64
302-N150-FR	1.99	19.62	19.60	19.52	19.26	20.96	20.93	20.92	20.46
302-N150-FR	2.00	77.49	77.36	76.86	75.35	88.97	88.95	88.85	88.32
302-N150-FR	4.00	159.31	158.75	156.15	149.66	196.16	196.06	195.80	194.57

Table A Web crippling strengths of austenitic stainless steel sections predicted from finite element analysis (c) *x/h* for offset circular web opening case

Specimen	Thickness	Unfastened FEA load per web, P_{FEA}				Fastened FEA load per web, P_{FEA}			
	t	*A* (0)	*A* (0.2)	*A* (0.4)	*A* (0.6)	*A* (0)	*A* (0.2)	*A* (0.4)	*A* (0.6)
	(mm)	(kN)	(kN)	(kN)	(kN)	(kN)	(kN)	(kN)	(kN)
142-N100-A0-FR	1.27	8.17	8.17	8.17	8.17	8.85	8.85	8.85	8.85
142-N100-A0.2-FR	1.27	8.01	8.02	8.03	8.07	8.81	8.82	8.83	8.83
142-N100-A0.4-FR	1.27	7.77	7.78	7.79	7.89	8.71	8.72	8.74	8.78
142-N100-A0.6-FR	1.27	7.26	7.32	7.53	7.73	8.24	8.34	8.54	8.69
142-N100-A0.8-FR	1.27	6.24	6.80	7.21	7.53	---	---	---	---
142-N120-A0-FR	1.27	8.65	8.65	8.65	8.65	9.42	9.42	9.42	9.42
142-N120-A0.2-FR	1.27	8.50	8.56	8.57	8.60	9.38	9.39	9.40	9.41
142-N120-A0.4-FR	1.27	8.20	8.25	8.34	8.45	9.26	9.28	9.30	9.36
142-N120-A0.6-FR	1.27	7.66	7.79	8.04	8.26	8.78	8.94	9.16	9.28
142-N120-A0.8-FR	1.27	6.57	7.14	7.63	7.98	8.05	8.41	8.96	9.19
142-N150-A0-FR	1.28	9.43	9.43	9.43	9.43	10.17	10.17	10.17	10.17
142-N150-A0.2-FR	1.28	9.28	9.31	9.33	9.36	10.12	10.13	10.14	10.16
142-N150-A0.4-FR	1.28	8.93	8.94	9.06	9.19	9.95	9.97	10.06	10.12
142-N150-A0.6-FR	1.28	8.13	8.38	8.68	8.94	9.37	9.64	9.91	10.06
142-N150-A0.8-FR	1.28	7.05	7.61	8.09	8.45	8.17	8.97	9.55	9.89
202-N100-A0-FR	1.39	9.33	9.33	9.33	9.33	9.61	9.61	9.61	9.61
202-N100-A0.2-FR	1.39	9.18	9.20	9.21	9.23	8.53	9.55	9.57	9.60
202-N100-A0.4-FR	1.39	8.83	8.84	8.94	9.06	8.93	8.94	9.07	9.25
202-N100-A0.6-FR	1.39	8.13	8.29	8.54	8.78	8.31	8.40	8.84	9.05
202-N120-A0-FR	1.39	9.91	9.91	9.91	9.91	10.82	10.82	10.82	10.82
202-N120-A0.2-FR	1.39	9.76	9.79	9.81	9.83	10.74	10.77	10.79	10.81
202-N120-A0.4-FR	1.39	9.36	9.37	9.49	9.62	10.52	10.52	10.62	10.74
202-N120-A0.6-FR	1.39	8.42	8.66	8.99	9.30	9.92	10.15	10.49	10.64
202-N150-A0-FR	1.45	11.63	11.63	11.63	11.63	11.90	11.90	11.90	11.90
202-N150-A0.2-FR	1.45	11.47	11.49	11.51	11.55	11.85	11.86	11.88	11.89
202-N150-A0.4-FR	1.45	10.86	10.92	11.09	11.26	11.52	11.60	11.78	11.84
202-N150-A0.6-FR	1.45	9.67	9.98	10.37	10.76	10.73	11.09	11.56	11.71
302-N100-A0-FR	1.98	17.94	17.94	17.94	17.94	18.62	18.62	18.62	18.62
302-N100-A0.2-FR	1.98	17.73	17.76	17.79	17.84	18.54	18.57	18.59	18.61
302-N120-A0-FR	1.96	18.67	18.67	18.67	18.67	19.27	19.27	19.27	19.27

Table A Continued
(c) Continued

Specimen	Thickness	Unfastened FEA load per web, P_{FEA}				Fastened FEA load per web, P_{FEA}			
	t	A (0)	A (0.2)	A (0.4)	A (0.6)	A (0)	A (0.2)	A (0.4)	A (0.6)
	(mm)	(kN)	(kN)	(kN)	(kN)	(kN)	(kN)	(kN)	(kN)
302-N120-A0.2-FR	1.96	18.50	18.54	18.59	18.63	19.23	19.24	19.52	19.63
302-N120-A0.4-FR	1.96	18.04	18.06	18.30	18.49	18.42	18.55	18.70	18.71
302-N120-A0.6-FR	1.96	16.87	17.75	18.72	19.43	18.08	18.15	18.22	18.39
302-N150-A0-FR	1.99	21.14	21.14	21.14	21.14	20.57	20.57	20.57	20.57
302-N150-A0.2-FR	1.99	19.97	21.00	21.05	21.10	20.49	20.51	20.52	20.54
302-N150-A0.4-FR	1.99	20.34	20.37	20.68	20.92	20.27	20.39	20.40	20.45
302-N150-A0.6-FR	1.99	18.56	19.15	19.99	20.58	19.03	19.75	19.88	20.16

Appendix B: Ferritic

Table B Web crippling strengths of ferritic stainless steel sections predicted from finite element analysis
(a) *a/h* for centred circular web opening case

Specimen	Thickness	Unfastened FEA load per web, P_{FEA}					Fastened FEA load per web, P_{FEA}				
	t	*A* (0)	*A* (0.2)	*A* (0.4)	*A* (0.6)	*A* (0.8)	*A* (0)	*A* (0.2)	*A* (0.4)	*A* (0.6)	*A* (0.8)
	(mm)	(kN)	(kN)	(kN)	(kN)	(kN)	(kN)	(kN)	(kN)	(kN)	(kN)
142-N100-FR	1.27	9.64	9.55	9.50	8.98	7.98	10.13	10.01	9.83	9.57	8.56
142-N100-FR	4.00	75.39	74.54	70.34	64.89	56.30	86.65	86.32	83.06	78.31	70.35
142-N100-FR	6.00	137.93	136.61	124.50	109.57	88.79	170.00	167.14	158.77	145.91	135.41
142-N120-FR	1.27	10.30	10.25	10.23	9.38	8.37	11.01	10.99	10.88	10.17	9.03
142-N120-FR	4.00	78.92	77.99	73.93	67.87	56.96	94.74	94.16	89.69	82.18	73.45
142-N120-FR	6.00	138.00	134.32	124.67	108.57	87.95	172.45	168.87	160.43	148.22	130.58
142-N150-FR	1.28	11.15	11.12	10.69	9.77	8.80	11.91	11.94	11.64	10.72	9.62
142-N150-FR	4.00	79.09	78.31	74.62	66.02	53.18	102.89	101.57	101.57	90.09	80.21
142-N150-FR	6.00	132.05	129.07	120.00	103.68	82.86	170.58	167.70	160.53	149.33	133.15
202-N100-FR	1.39	10.95	10.93	10.92	9.86	-	10.99	10.97	10.56	10.47	-
202-N100-FR	4.00	76.67	76.06	73.11	66.17	-	84.44	84.09	82.29	75.25	-
202-N100-FR	6.00	153.20	150.53	142.09	128.00	-	179.07	177.81	172.61	155.54	-
202-N120-FR	1.39	11.59	11.58	11.25	10.05	-	12.51	12.37	12.24	11.90	-
202-N120-FR	4.00	80.57	79.82	75.72	69.10	-	92.59	92.32	88.81	79.69	-
202-N120-FR	6.00	158.38	157.84	146.08	129.79	-	194.15	192.76	184.90	166.88	-
202-N150-FR	1.39	12.25	12.18	11.52	10.38	-	13.73	13.46	13.14	12.49	-
202-N150-FR	4.00	85.51	84.46	79.56	73.90	-	104.08	102.52	96.97	88.13	-
202-N150-FR	6.00	161.20	158.91	149.02	128.86	-	213.37	204.50	193.90	175.41	-
302-N100-FR	1.98	20.65	20.60	20.55	20.41	-	20.91	20.89	20.26	19.91	-
302-N100-FR	4.00	77.78	77.71	76.25	72.26	-	80.76	80.64	78.58	75.58	-
302-N100-FR	6.00	163.56	162.23	159.46	141.16	-	175.68	175.16	169.02	159.23	-
302-N120-FR	1.98	22.47	22.24	22.16	21.04	-	21.96	21.95	21.80	20.62	-
302-N120-FR	4.00	82.48	82.46	81.75	74.75	-	87.93	87.73	86.99	79.95	-
302-N120-FR	6.00	171.22	169.60	163.26	146.01	-	192.12	191.29	187.23	166.10	-
302-N150-FR	1.99	24.65	24.55	24.47	22.01	-	23.59	23.57	23.26	21.28	-
302-N150-FR	4.00	88.92	88.82	86.90	78.24	-	97.97	97.61	95.84	84.30	-
302-N150-FR	6.00	181.23	179.42	170.46	154.64	-	215.29	213.67	205.54	174.956	-

Table B Web crippling strengths of ferritic stainless steel sections predicted from finite element analysis
(b) *a/h* for offset circular web opening case

Specimen	Thickness	Unfastened FEA load per web, P_{FEA}				Fastened FEA load per web, P_{FEA}			
	t	A (0)	A (0.2)	A (0.4)	A (0.6)	A (0)	A (0.2)	A (0.4)	A (0.6)
	(mm)	(kN)	(kN)	(kN)	(kN)	(kN)	(kN)	(kN)	(kN)
142-N100-FR		9.54	9.53	9.48	9.40	10.18	10.17	10.16	10.15
142-N100-FR	4.00	75.44	75.36	75.06	74.56	86.75	86.73	86.71	86.69
142-N100-FR	6.00	135.73	135.39	134.40	132.63	170.00	169.78	168.93	159.64
142-N120-FR	1.27	10.28	10.27	10.18	10.02	11.01	10.99	10.98	10.96
142-N120-FR	4.00	78.98	78.87	78.50	77.69	94.82	94.78	94.76	94.74
142-N120-FR	6.00	137.05	136.63	135.45	133.41	172.45	172.20	171.01	160.33
142-N150-FR	1.28	11.14	11.10	10.94	10.61	11.95	11.93	11.91	11.88
142-N150-FR	4.00	79.05	78.84	78.31	77.34	102.50	102.49	102.38	102.05
142-N150-FR	6.00	131.75	131.24	129.91	127.68	170.58	170.31	169.05	160.25
202-N100-FR	1.39	10.74	10.67	10.44	9.83	11.61	11.59	11.57	11.50
202-N100-FR	4.00	76.62	76.48	76.03	75.16	84.49	84.47	84.44	84.41
202-N100-FR	6.00	153.08	152.73	151.58	148.79	179.11	179.08	179.05	179.01
202-N120-FR	1.39	11.40	11.29	10.88	10.03	11.89	11.86	11.82	11.70
202-N120-FR	4.00	80.53	80.37	79.81	78.62	92.59	92.58	92.54	92.50
202-N120-FR	6.00	157.32	156.91	155.42	151.66	194.15	194.11	194.04	190.53
202-N150-FR	1.39	12.08	11.88	11.27	10.49	13.75	13.74	13.69	13.52
202-N150-FR	4.00	85.49	85.29	84.57	82.58	104.47	103.42	103.39	103.26
202-N150-FR	6.00	161.15	160.58	158.72	154.05	207.25	206.87	205.31	192.39
302-N100-FR	1.98	19.02	19.00	18.94	18.81	20.93	20.91	20.87	20.78
302-N100-FR	2.00	77.78	77.69	77.34	76.55	80.83	80.80	80.75	80.69
302-N100-FR	4.00	163.58	163.28	162.22	158.58	175.77	175.73	175.71	175.67
302-N120-FR	1.98	20.63	20.52	20.43	20.18	21.96	21.95	21.93	21.84
302-N120-FR	2.00	82.48	82.37	81.86	80.59	87.97	87.95	87.90	87.81
302-N120-FR	4.00	171.25	170.87	169.26	160.22	192.17	192.16	192.13	192.06
302-N150-FR	1.99	22.47	22.45	22.25	21.50	23.59	23.59	23.56	23.41
302-N150-FR	2.00	88.79	88.60	87.89	85.33	97.97	97.96	97.94	97.75
302-N150-FR	4.00	181.04	180.29	176.64	166.49	215.31	215.30	215.29	215.25

Table B Web crippling strengths of ferritic stainless steel sections predicted from finite element analysis (c) *x/h* for offset circular web opening case

Specimen	Thickness	Unfastened FEA load per web, P_{FEA}				Fastened FEA load per web, P_{FEA}			
	t	*X* (0)	*X* (0.2)	*X* (0.4)	*X* (0.6)	*X* (0)	*X* (0.2)	*X* (0.4)	*X* (0.6)
	(mm)	(kN)	(kN)	(kN)	(kN)	(kN)	(kN)	(kN)	(kN)
142-N100-A0-FR	1.27	9.19	9.19	9.19	9.19	9.67	9.67	9.67	9.67
142-N100-A0.2-FR	1.27	9.10	9.11	9.12	9.15	9.62	9.64	9.65	9.66
142-N100-A0.4-FR	1.27	8.83	8.85	8.95	9.05	9.58	9.59	9.61	9.65
142-N100-A0.6-FR	1.27	8.31	8.45	8.69	8.91	9.21	9.34	9.53	9.63
142-N100-A0.8-FR	1.27	7.14	7.76	8.23	8.62	---	---	---	---
142-N120-A0-FR	1.27	9.96	9.96	9.96	9.96	10.56	10.56	10.56	10.56
142-N120-A0.2-FR	1.27	9.84	9.86	9.87	9.90	10.51	10.52	10.52	10.54
142-N120-A0.4-FR	1.27	9.48	9.51	9.63	9.75	10.36	10.38	10.43	10.50
142-N120-A0.6-FR	1.27	8.71	8.92	9.22	9.50	9.83	10.04	10.30	10.45
142-N120-A0.8-FR	1.27	7.46	8.09	8.56	8.90	8.32	9.31	10.04	10.39
142-N150-A0-FR	1.28	11.29	11.29	11.29	11.29	11.57	11.57	11.57	11.57
142-N150-A0.2-FR	1.28	10.72	10.75	10.77	10.81	11.49	11.50	11.53	11.55
142-N150-A0.4-FR	1.28	10.18	10.21	10.78	10.94	11.23	11.25	11.39	11.50
142-N150-A0.6-FR	1.28	9.19	9.48	9.82	10.13	10.49	10.78	11.16	11.40
142-N150-A0.8-FR	1.28	7.94	8.53	8.99	9.25	8.99	9.87	10.62	11.18
202-N100-A0-FR	1.39	10.61	10.61	10.61	10.61	10.58	10.58	10.58	10.58
202-N100-A0.2-FR	1.39	10.46	10.50	10.51	10.54	10.53	10.55	10.57	10.58
202-N100-A0.4-FR	1.39	10.01	10.03	10.16	10.31	9.90	9.92	10.05	10.14
202-N100-A0.6-FR	1.39	8.84	9.13	9.44	9.74	9.55	9.72	9.88	10.06
202-N120-A0-FR	1.39	11.36	11.36	11.36	11.36	12.10	12.10	12.10	12.10
202-N120-A0.2-FR	1.39	11.17	11.20	11.20	11.23	12.05	12.06	12.07	12.05
202-N120-A0.4-FR	1.39	10.38	10.46	10.63	10.80	11.76	11.77	11.94	12.05
202-N120-A0.6-FR	1.39	9.06	9.35	9.65	9.93	11.04	11.28	11.70	11.98
202-N150-A0-FR	1.45	13.16	13.16	13.16	13.16	13.45	13.45	13.45	13.45
202-N150-A0.2-FR	1.45	12.85	12.88	12.89	12.93	13.34	13.35	13.40	13.44
202-N150-A0.4-FR	1.45	11.76	11.85	12.03	12.24	12.86	12.91	13.16	13.35
202-N150-A0.6-FR	1.45	10.29	10.58	10.89	11.22	11.86	12.21	12.75	13.21
302-N100-A0-FR	1.98	20.09	20.09	20.09	20.09	20.12	20.12	20.12	20.12
302-N100-A0.2-FR	1.98	19.94	19.99	20.03	20.07	20.05	20.09	20.11	20.12
302-N120-A0-FR	1.96	21.37	21.37	21.37	21.37	21.36	21.36	21.36	21.36
302-N120-A0.2-FR	1.96	21.20	21.22	21.27	21.32	21.34	21.34	21.33	21.34

Table B Continued
(c) Continued

Specimen	Thickness	Unfastened FEA load per web, P_{FEA}				Fastened FEA load per web, P_{FEA}			
	t	X (0)	X (0.2)	X (0.4)	X (0.6)	X (0)	X (0.2)	X (0.4)	X (0.6)
	(mm)	(kN)	(kN)	(kN)	(kN)	(kN)	(kN)	(kN)	(kN)
302-N120-A0.4-FR	1.96	20.51	20.53	20.82	21.10	20.36	20.56	20.68	20.67
302-N120-A0.6-FR	1.96	18.25	18.88	19.79	20.63	19.95	20.07	20.17	20.34
302-N150-A0-FR	1.99	24.20	24.20	24.20	24.20	23.17	23.17	23.17	23.17
302-N150-A0.2-FR	1.99	23.91	23.94	24.01	24.10	23.12	23.13	23.15	23.19
302-N150-A0.4-FR	1.99	22.58	22.71	23.12	23.60	22.42	22.80	22.97	22.97
302-N150-A0.6-FR	1.99	19.85	20.53	21.54	22.57	20.73	21.73	22.16	22.37